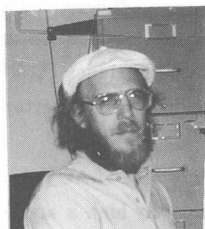


## SPIN STRUCTURE FUNCTIONS AT SLAC

P. Bosted  
(The E143 Collaboration)  
American University, Washington DC 20016



## Abstract

A brief review is given of nucleon spin structure function measurements at SLAC. Highlighted are recent measurements of the  $Q^2$  dependence of  $g_1^p$  and  $g_1^d$ . The assumption that  $g_1$  and  $F_1$  have approximately the same  $Q^2$ -dependence has been found to be consistent with all available data in the deep inelastic region  $Q^2 > 1$  ( $\text{GeV}/c$ ) $^2$ , although significant deviations from this assumption are found at lower  $Q^2$ . Global fits to the data with and without a possible  $Q^2$  dependence to  $g_1/F_1$  provide a useful parameterization of available data, and validate previous conclusions that the fundamental Bjorken sum rule is satisfied, and that the net quark helicity of the nucleon is less than expected in the simple relativistic parton model.

The longitudinal and transverse spin-dependent structure functions  $g_1(x, Q^2)$  and  $g_2(x, Q^2)$  for deep-inelastic lepton-nucleon scattering have become increasingly important in unraveling the quark and gluon spin structure of the proton and neutron. The  $g_1$  structure function depends both on  $x$ , the fractional momentum carried by the struck parton, and on  $Q^2$ , the four-momentum transfer squared of the virtual photons used as a probe of nucleon structure. Of particular interest are the fixed- $Q^2$  integrals  $\Gamma_1^p(Q^2) = \int_0^1 g_1^p(x, Q^2) dx$  for the proton and  $\Gamma_1^n(Q^2) = \int_0^1 g_1^n(x, Q^2) dx$  for the neutron. These integrals are directly related to the net quark helicity  $\Delta q$  in the nucleon. Measurements<sup>1-8)</sup> of  $\Gamma_1^p$ ,  $\Gamma_1^d$ , and  $\Gamma_1^n$  have found  $\Delta q \approx 0.3$ , significantly less than a prediction<sup>9)</sup> that  $\Delta q = 0.58$  assuming zero net strange quark helicity and SU(3) flavor symmetry in the baryon octet. A fundamental sum rule originally derived from current algebra by Bjorken<sup>10)</sup> predicts the difference  $\Gamma_1^p(Q^2) - \Gamma_1^n(Q^2)$ . Recent measurements are in agreement with this sum rule prediction when perturbative QCD (pQCD) corrections<sup>11)</sup> are included.

Measurements of spin structure functions at SLAC began in 1977 with the E80<sup>1)</sup> and E130<sup>2)</sup> experiments, which measured  $g_1^p$  at relatively high  $x$  and low  $Q^2$ , due to the maximum beam energy of 20 GeV. Improvements in target technology and the development at SLAC of a high intensity, high polarization electron beam allowed a new generation of experiments to begin in 1992. The first experiment, E142<sup>8)</sup>, used a  ${}^3\text{He}$  target with beam energies of 16 to 25 GeV and 40% polarization to make the first measurement of the neutron spin structure function  $g_1^n$ . The final results<sup>12)</sup> of this experiment differ somewhat from the initial publication due to many improvements in the analysis, and are expected to be submitted for publication shortly. In 1993, the E143 experiment measured  $g_1^p$ ,  $g_1^n$ ,  $g_2^p$ , and  $g_2^n$  using polarized  $\text{NH}_3$  and  $\text{ND}_3$  targets and an 83% polarized electron beam with energies up to 29 GeV. This allowed a wide range of both  $x$  and  $Q^2$  to be explored in a single target, and the first precise measurements<sup>13)</sup> of  $g_2$ . More details of the  $Q^2$  dependence of the E143 results<sup>14)</sup> are given below. Finally, experiment E154 returned to the  ${}^3\text{He}$  target in late 1995, now with an increased beam energy of 48.5 GeV, and a higher beam polarization of 83%. This allowed lower values of  $x$  (down to 0.015) to be probed than in E142, and improvements in the target and beam parameters allowed approximately a factor of three smaller statistical errors. Preliminary results were not yet available at the time of the Moriond meeting.

The rest of this contribution focuses on a more detailed discussion of a recent study<sup>14)</sup> by the E143 Collaboration of the  $Q^2$  dependence of  $g_1$ . There are two main reasons for measuring  $g_1$  over a wide range of  $x$  and  $Q^2$ . The first is that experiments make measurements at fixed beam energies rather than at fixed  $Q^2$ . To evaluate first moment integrals of  $g_1(x, Q^2)$  at constant  $Q^2$  [typically between 2 and 10  $(\text{GeV}/c)^2$ ], extrapolations are needed. The second motivation is that the kinematic dependence of  $g_1$  can be used to obtain the underlying nucleon polarized quark and gluon distribution functions. According to the GLAP equations<sup>15)</sup>,  $g_1$  is expected to

evolve logarithmically with  $Q^2$ , increasing with  $Q^2$  at low  $x$ , and decreasing with  $Q^2$  at high  $x$ . A similar  $Q^2$ -dependence has been observed in the spin-averaged structure functions  $F_1(x, Q^2)$  and  $F_2(x, Q^2)$ , so in first approximation the ratio  $g_1/F_1$  should be independent of  $Q^2$  at fixed  $x$ . The detailed behavior of  $g_1/F_1$  is sensitive to the underlying polarized quark and gluon densities, as well as to possible higher twist effects, expected to be proportional to  $C(x)/Q^2$ ,  $D(x)/Q^4$ , etc., where  $C(x)$  and  $D(x)$  are unknown functions.

The analysis principally used the E143 data, taken at beam energies of 9.7, 16.2, and 29 GeV. Data at all energies were taken at scattering angles of  $4.5^\circ$  and  $7^\circ$ . The ratio of polarized to unpolarized structure functions was determined from measured longitudinal asymmetries  $A_{\parallel}$  using

$$g_1/F_1 = A_{\parallel}/d + (g_2/F_1)[(2Mx)/(2E - \nu)] , \quad (1)$$

where  $d = [(1 - \epsilon)(2 - y)]/\{y[1 + \epsilon R(x, Q^2)]\}$ ,  $y = \nu/E$ ,  $\nu = E - E'$ ,  $E'$  is the scattered electron energy,  $\epsilon^{-1} = 1 + 2[1 + \gamma^{-2}]\tan^2(\theta/2)$ ,  $\gamma^2 = Q^2/\nu^2$ ,  $\theta$  is the electron scattering angle,  $M$  is the nucleon mass, and  $R(x, Q^2) = [F_2(x, Q^2)(1 + \gamma^2)]/[2xF_1(x, Q^2)] - 1$  is typically 0.2 for the kinematics of this experiment<sup>16)</sup>. For the contribution of the transverse spin structure function  $g_2$ , the twist-two model of Wandzura and Wilczek<sup>17)</sup> ( $g_2^{WW}$ ) was used. Using other reasonable models for  $g_2$  (such as  $g_2 = 0$ ) has relatively little impact on the results for  $g_1$  due to the factor  $2Mx/(2E - \nu)$  in Eq. 1.

The data analysis was essentially identical to that reported for the E143 29 GeV data<sup>5,7)</sup>, with  $A_{\parallel}$  calculated from the difference over the sum of rates for scattering longitudinally polarized electrons with spin either parallel or anti-parallel to polarized protons or deuterons in a cryogenic ammonia target. The most important corrections made were for the beam polarization (typically  $0.85 \pm 0.02$ ), target polarization (typically  $0.65 \pm 0.017$  for  $\text{NH}_3$ ,  $0.25 \pm 0.011$  for  $\text{ND}_3$ ), fraction of polarizable nucleons (0.12 to 0.17 for  $\text{NH}_3$ , 0.22 to 0.24 for  $\text{ND}_3$ ), and for contributions from polarized nitrogen atoms. Radiative corrections were calculated<sup>18)</sup> using iterated global fits to all data. The 29 GeV data used here differ slightly from the previously published results<sup>5,7)</sup> due to the new radiative corrections, the inclusion of more data runs, and improved measurements of the polarization of the target and beam. Data in the resonance region defined by missing mass  $W < 1.8$  GeV were not included in the present analysis, but those for  $Q^2$  below the traditional deep-inelastic cutoff of  $Q^2 = 1$  (GeV/c)<sup>2</sup> were kept.

The E143 results for  $g_1^p/F_1^p$  and  $g_1^d/F_1^d$  are shown in Fig. 1, at eight values of  $x$ . Data from other experiments<sup>1-4,6)</sup> are plotted using published longitudinal asymmetries  $A_{\parallel}$  and the same model for  $R(x, Q^2)$  and  $g_2$  as for the E143 data. Improved radiative corrections have been applied to the E80 and E130 results. Only statistical errors have been plotted. For the E143 experiment, most systematic errors (beam polarization, target polarization, fraction of polarizable nucleons in the target) for a given target are common to all data and correspond to an overall normalization error of about 5% for the proton data and 6% for the deuteron

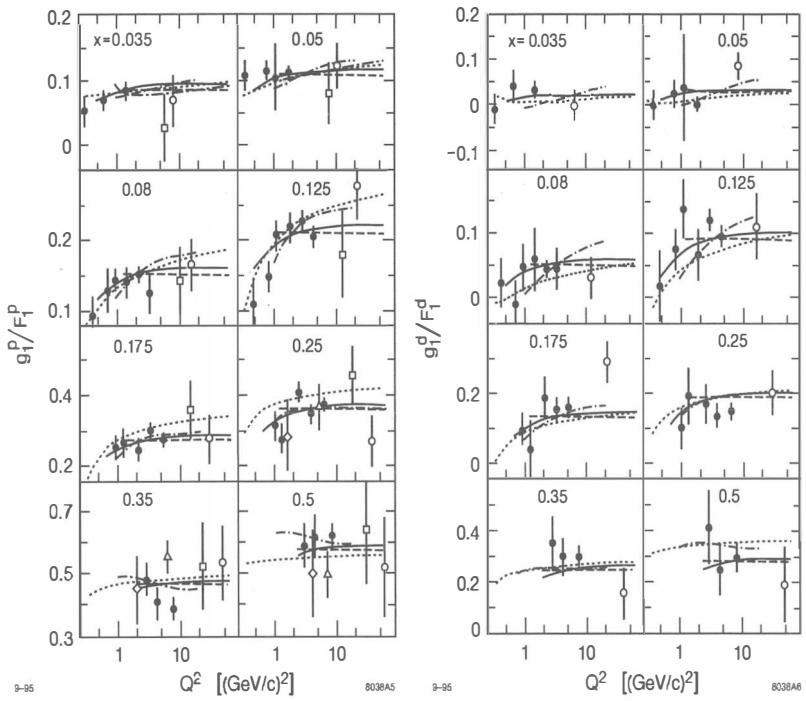


Figure 1. Ratios  $g_1^p/F_1^p$  (left) and  $g_1^d/F_1^d$  (right) extracted from experiments assuming the  $g_2^{WW}$  model for  $g_2$ . The errors are statistical only. Data are from E143<sup>14)</sup> (solid circles), SLAC E80<sup>1)</sup> (diamonds), SLAC E130<sup>2)</sup> (triangles), EMC<sup>3)</sup> (squares), and SMC<sup>4)</sup> (open circles). The dashed and solid curves correspond to global fits II ( $g_1^p/F_1^p$   $Q^2$ -independent) and III ( $g_1^p/F_1^p$   $Q^2$ -dependent). Representative NLO pQCD fits from Refs. 19 and 20 are shown as the dot-dashed and dotted curves, respectively.

data. The remaining systematic errors (radiative corrections, model uncertainties for  $R(x, Q^2)$ , resolution corrections) vary smoothly with  $x$  in a locally correlated fashion, ranging from a few percent for moderate  $x$  bins, up to 15% for the highest and lowest  $x$  bins at  $E = 29$  GeV. For all data, the statistical errors dominate over the point-to-point systematic error.

The most striking feature of the data is that  $g_1/F_1$  is approximately independent of  $Q^2$  at fixed  $x$ , although there is a noticeable trend for the ratio to decrease for  $Q^2 < 1$  (GeV/c) $^2$ . To quantify the possible significance of this trend, the data in each  $x$  bin were fit with the form  $g_1/F_1 = a(1 + C/Q^2)$ . The results for the  $C$  coefficients are shown in Fig. 2 for all  $Q^2$  [ $Q^2 > 0.3$  (GeV/c) $^2$ ] (circles) and for  $Q^2 > 1$  (GeV/c) $^2$  (squares). The coefficients indicate significantly negative values for  $C$  at intermediate values of  $x$  for the fits over all  $Q^2$ . The errors are much larger when data with  $Q^2 < 1$  (GeV/c) $^2$  are excluded, and the resulting coefficients are consistent with no  $Q^2$ -dependence to  $g_1/F_1$  ( $C = 0$ ). There is no evidence for a significant

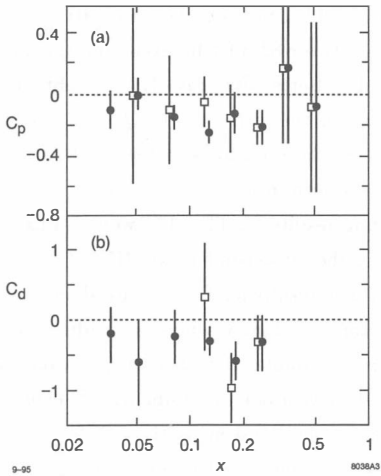


Figure 2. Coefficients  $C$  for fits to  $g_1/F_1$  at fixed  $x$  of the form  $a(1+C/Q^2)$  for (a) proton and (b) deuteron. Solid circles are fits to all data [ $Q^2 > 0.3$   $(\text{GeV}/c)^2$ ], and open squares are fits only to data with  $Q^2 > 1$   $(\text{GeV}/c)^2$ .

$x$ -dependence to  $C$ .

Shown in Fig. 1 as the dot-dashed curves are the low- $Q^2$  predictions from a representative global NLO pQCD fit<sup>19)</sup> to all proton and deuteron data excluding those at the 9.7 GeV and 16.2 GeV beam energies of E143. This curve has a relatively polarized gluon strength. This group<sup>19)</sup> finds considerably less  $Q^2$  dependence to  $g_1/F_1$  when a minimal polarized gluon strength is used than when a maximal strength is chosen. Another group has made NLO pQCD fits to proton, deuteron, and neutron data using different constraints on the underlying parton distribution functions<sup>20)</sup>, examining the sensitivity to SU(3) symmetry breaking in the baryon  $\beta$  decays. The results for their standard set are shown as the dotted curves in Fig. 1. Both groups predict that  $g_1^p/F_1^p$  increases with  $Q^2$  in the moderate  $x$  range ( $0.03 < x < 0.3$ ), in agreement with the trend of the data when the E143  $E = 9.7$  and  $E = 16.2$  results (not included in their fits) are considered.

The E143 group also performed simple global fits to the data, both in order to have a practical parameterization (needed, for example, in making radiative corrections to the data), and to examine the possible effects of  $Q^2$  dependence on the first moments  $\Gamma_1$ . Data points from SMC<sup>4,6)</sup> at  $x < 0.035$ , not shown in Fig. 1, were included in the fits. The first fits (case I) are of the  $Q^2$ -independent form  $g_1/F_1 = ax^\alpha(1+bx+cx^2)$ , with the constraint that  $A_1 = g_1/F_1 - \gamma^2 g_2^{WW}/F_1 \rightarrow 1$  for  $x \rightarrow 1$  at  $Q^2 = 2$   $(\text{GeV}/c)^2$ . The fits to all the proton and

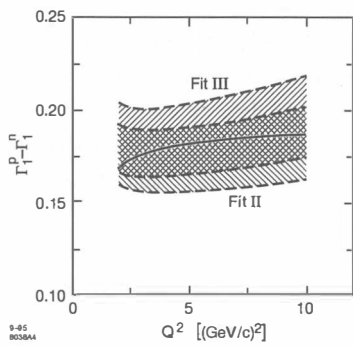


Figure 3. Evaluations of  $\Gamma_1^p - \Gamma_1^n$  from the  $Q^2$ -independent fits II (lower band) and  $Q^2$ -dependent fits III (upper band). The errors include both statistical and systematic contributions and are indicated by the widths of the bands. The solid curve is the prediction of the Bjorken sum rule with third-order QCD corrections.

deuteron data are acceptable (combined  $\chi^2 = 125$  for 104 d.f.), but the fits systematically lie above the lowest  $Q^2$  points. The fits are improved ( $\chi^2 = 94$  for 82 d.f.) by excluding the data for  $Q^2 < 1$  ( $\text{GeV}/c^2$ ) (case II, dashed curves in Fig. 1). Better fits (case III) are obtained by introducing an overall multiplicative correction term of the form  $(1 + C/Q^2)$  to account for the low  $Q^2$  data ( $\chi^2 = 104$  for 102 d.f.), as shown by the solid lines in Fig. 1. Using an  $x$ -independent value of  $C$  is reasonable given the results shown in Fig. 2.

The first moments  $\Gamma_1^p$  and  $\Gamma_1^d$ , and the corresponding results for  $\Gamma_1^p - \Gamma_1^n$ , were evaluated using the  $Q^2$ -independent fits II ( $Q^2 > 1$  ( $\text{GeV}/c^2$ )) and the  $Q^2$ -dependent fits III (all  $Q^2$ ). A global fit<sup>16,21</sup> was used for  $F_1$  to obtain  $g_1$  from  $g_1/F_1$ . The results for  $\Gamma_1^p - \Gamma_1^n$  are shown as a function of  $Q^2$  as the lower (fit II) and upper (fit III) bands in Fig. 3, where the width of the band reflects the combined statistical and systematic error estimate. Both fits are in reasonable agreement with the Bjorken sum rule, shown as the solid curve, evaluated using  $\alpha_s(Q^2)$  evolved in  $Q^2$  from  $\alpha_s(M_Z) = 0.117 \pm 0.005$ , with QCD corrections<sup>11</sup> taken to third order in  $\alpha_s$ . Alternatively, if the sum rule is assumed to be correct, the measured  $\Gamma_1^p(Q^2) - \Gamma_1^n(Q^2)$  can be used to determine the strong coupling  $\alpha_s$ . The case II ( $Q^2$ -independent  $g_1/F_1$ ) fits to the proton and deuteron data integrated at  $Q^2 = 3$  ( $\text{GeV}/c^2$ ) yield  $\alpha_s(M_Z) = 0.119^{+0.007}_{-0.019}$ , while the case III ( $Q^2$ -dependent  $g_1/F_1$ ) fits yield  $\alpha_s(M_Z) = 0.113^{+0.011}_{-0.035}$ , both in agreement with the world average result of 0.117.

Also examined is the sensitivity to the possible  $Q^2$  dependence of  $g_1/F_1$  of the net quark helicity  $\Delta q$  extracted from global fits to the data.  $\Delta q$  was computed using  $F + D = 1.2573 \pm 0.0028$ , and  $F/D = 0.575 \pm 0.016$ , extracted assuming SU(3) flavor symmetry in the baryon octet. At  $Q^2 = 3$  ( $\text{GeV}/c^2$ ),  $\Delta q = 0.34 \pm 0.09$  was obtained for global proton fit II, and  $\Delta q = 0.36 \pm 0.10$  was obtained for proton fit III, somewhat higher than  $\Delta q = 0.27 \pm 0.10$ , obtained using the previous analysis of the E143  $E = 29$  GeV data only<sup>5</sup>, which assumed  $g_1/F_1$  independent of  $Q^2$ . For the deuteron fits,  $\Delta q = 0.35 \pm 0.05$  for fit II, and  $\Delta q = 0.34 \pm 0.05$  for fit III, again somewhat higher than the previous deuteron analysis<sup>7</sup>  $\Delta q = 0.30 \pm 0.06$ , but in good agreement with the new proton results.

In summary, the assumption that  $g_1$  and  $F_1$  have approximately the same  $Q^2$ -dependence has been found to be consistent with all available data in the deep inelastic region  $Q^2 > 1$  ( $\text{GeV}/c^2$ ), although significant deviations from this assumption are found at lower  $Q^2$ . Global fits to the data with and without a possible  $Q^2$  dependence to  $g_1/F_1$  provide a useful parameterization of available data, and validate previous conclusions that the fundamental Bjorken sum rule is satisfied, and that the net quark helicity content of the nucleon is less than expected in the simple relativistic parton model.

1. SLAC E80, M. J. Alguard et al., Phys. Rev. Lett. 37 (1976) 1261; 41 (1978) 70.
2. SLAC E130, G. Baum et al., Phys. Rev. Lett. 51 (1983) 1135.

3. EMC, J. Ashman et al., *Phys. Lett.* B206 (1988) 364; *Nucl. Phys.* B328 (1989) 1.
4. SMC, D. Adams et al., *Phys. Lett.* B329 (1994) 399.
5. SLAC E143, K. Abe et al., *Phys. Rev. Lett.* 74 (1995) 346.
6. SMC, D. Adams et al., *Phys. Lett.* B357 (1995) 248.
7. SLAC E143, K. Abe et al., *Phys. Rev. Lett.* 75 (1995) 25.
8. SLAC E142, P. L. Anthony et al., *Phys. Rev. Lett.* 71 (1993) 959.
9. J. Ellis and R. Jaffe, *Phys. Rev. D* 9 (1974) 1444; D 10 (1974) 1669 (E).
10. J. D. Bjorken, *Phys. Rev.* 148 (1966) 1467; *Phys. Rev. D* 1 (1970) 1376.
11. S. A. Larin and J.A.M. Vermaseren, *Phys. Lett.* B259 (1991) 345 and references therein.
12. J. Dunne, PhD thesis, The American University (1995); D. Kawall, PhD thesis, Stanford University (1995).
13. SLAC E143, K. Abe et al., *Phys. Rev. Lett.* 76 (1995) 587.
14. SLAC E143, K. Abe et al., *Phys. Lett.* B364 (1995), 61.
15. G. Altarelli and G. Parisi, *Nucl. Phys.* B126 (1977) 298; V. N. Gribov and L. N. Lipatov, *Yad. Fiz.* 15 (1972) 781 [*Sov. J. Nucl. Phys.* 15 (1972) 438].
16. L. W. Whitlow et al., *Phys. Lett.* B250 (1990) 193.
17. S. Wandzura and F. Wilczek, *Phys. Lett.* B72 (1977) 195.
18. T. V. Kuchto and N. M. Shumeiko, *Nucl. Phys.* B219 (1983) 412; I. V. Akusevich and N. M. Shumeiko, *J. Phys. G* 20 (1994) 513.
19. R. D. Ball, S. Forte, and G. Ridolfi, *Nucl. Phys.* B444 (1995) 287; and CERN-TH/95-266 (1995).
20. M. Glück, E. Reya, M. Stratmann, and W. Vogelsang, *Phys. Rev. D* 53, 4775 (1996).
21. NMC, P. Amaudruz et al., *Phys. Lett.* B295 (1992) 159.